



# Monsoon-Driven Geomorphological Changes Along the West Coast of Sri Lanka: A Combined Approach Utilizing ‘CoastSat’ and Google Earth Engine

Gunasinghage Prasadh Gunasinghe<sup>1,2</sup> · Nalin Prasanna Ratnayake<sup>1</sup> · Amila Sandaruwan Ratnayake<sup>3</sup> · G. V. I. Samaradivakara<sup>1</sup> · Nimila Praneeth Dushyantha<sup>3</sup> · Ravindra Jayaratne<sup>4</sup> · Kodithuwakka Arachchige Dinusha<sup>2</sup> · Akalanka Silva<sup>5</sup>

Received: 7 December 2021 / Revised: 18 April 2022 / Accepted: 2 May 2022 / Published online: 7 July 2022

© The Author(s), under exclusive licence to Korea Institute of Ocean Science & Technology (KIOST) and the Korean Society of Oceanography (KSO) and Springer Nature B.V. 2022

## Abstract

Long-term field monitoring of shoreline changes is time-consuming, expensive, and labor-intensive. Instead, satellite images can be used as an alternative method to collect field data. The time-series satellite images are available at any location in the world that can be processed with the Google Earth Engine cloud environment. This study primarily focuses on shoreline change detection and describing the coastal geomorphology of three urban beaches on the west coast of Sri Lanka. The study extended from 2015 to 2021 during which large-scale coastal development projects were carried out in the study area. The ‘CoastSat’ toolkit was used to extract the time-series of shoreline positions. Time-series shoreline position obtained through ‘CoastSat’ was compared with the field measurements carried out using the Global Navigation Satellite System technique with a horizontal accuracy of 7 mm. The results indicate that the average horizontal difference of shoreline positions obtained by ‘CoastSat’ and field observation was  $7.5 \pm 1$  m in Agulana-Ratmalana on 19 August 2019, and was  $8.3 \pm 1$  m in Kalutara on 29 July 2020. The extracted shoreline changes show erosion and deposition patterns affected by monsoon seasonality and anthropogenic events. The results further show that North of Mount Lavinia Beach was accreted from 18 to 27 m, while South of Mount Lavinia Beach was eroded from 12 to 17 m. Accretion was mainly due to sand nourishment in the area during the 1st quarter of 2020. Furthermore, Agulana-Ratmalana Beach predominantly accreted from 22 to 30 m, while the northernmost transect (AR1) had a steady-state beach condition. This was again due to nourished sand during the 1st quarter of 2020. In contrast, accretion and erosion trends in Kalutara Beach are mainly due to the breakup of the river mouth sand bar to control flooding by the artificial cutting open of the sand spit bar in 2017. The transect (KL2) near the broken sand spit bar at the north of Kalutara shows severe erosion (56 m), since northward longshore transport of sediment has stopped with the breakage of the sand spit bar. In contrast, Kalutara south transects show an accretion to steady-state condition due to the existing hard engineering structures. Consequently, the study suggests that the CoastSat: A Google Earth Engine-enabled Python toolkit can be used to extract shoreline positions and to detect medium-to-large-scale coastline changes with appropriate tidal corrections, when and where there are no long-term coastal field measurements available. This method could be adapted to any coastal area in the world for acceptable shoreline detection that would be very useful for planning and evaluating coastal management strategies.

**Keywords** Beach nourishment · Coastal erosion and accretion · Monsoon · Nearshore currents · Shoreline changes

✉ Gunasinghage Prasadh Gunasinghe  
prasadh@kdu.ac.lk

<sup>1</sup> Department of Earth Resources Engineering, Faculty of Engineering, University of Moratuwa, Moratuwa 10400, Sri Lanka

<sup>2</sup> Department of Spatial Sciences, KDU Southern Campus, Sewanagala 70250, Sri Lanka

<sup>3</sup> Department of Applied Earth Sciences, Faculty of Applied Sciences, Uva Wellassa University, Passara 90500, Sri Lanka

<sup>4</sup> School of Architecture Computing and Engineering, University of East London, London E162RD, UK

<sup>5</sup> Department of Construction Technology, Wayamba University of Sri Lanka, Kuliypitiya 60200, Sri Lanka

## 1 Introduction

The highest intersection line of land and sea at a certain tidal elevation is considered as ‘shoreline’, and it is vital to demarcate the land-seawater boundary. An instantaneous shoreline can be defined as the location of the land–seawater boundary at a given time (Gens 2010). Under various circumstances, the different types of shoreline boundaries, such as wet–dry boundary, vegetation line, high tide line, and mean sea level (MSL), are also considered as the shoreline (Boak and Turner 2005; Ratnayake et al. 2019). Since shoreline is a fundamental feature of any coastal zone, shoreline changes have paramount importance in coastal zone management and engineering designs. The shoreline change is a function of beach erosion and accretion, which is influenced by factors, such as waves, tidal variations, natural hazards, anthropogenic impacts, sediment supply, littoral drift, sea-level rise due to climate change, hydrodynamics of the nearshore area, river mouth processes, and nature of the coastal landforms (Amalan et al. 2018; Kumar and Jayappa 2009; Lee 2014; Lee et al. 2019; Niya et al. 2013; Scott 2005). Since shoreline is highly dynamic, continuous investigations and monitoring are required for comprehensive analysis of shoreline changes and maintenance of sound coastal management systems (Bouchahma and Yan 2012; Chand and Acharya 2010; Fenster et al. 2001). However, continuous field investigations are time-consuming, expensive, and labor-intensive (Li et al. 2001; Natesan et al. 2013; Warnasuriya et al. 2015, 2018). To overcome these difficulties, remote-sensing (RS) technology can be adapted to monitor long-term shoreline changes. These techniques comprise several advantages, such as cost-effectiveness, minimizing manual errors, and availability of temporal data (Ali and Narayana 2015; Alicandro et al. 2019; Li et al. 2002; Specht et al. 2020).

Sri Lanka has a 1620 km-long coastal zone around the country, which features sandy beaches, estuaries, lagoons, salt marshes, coral reefs, and dunes along with significant biodiversity. These resources help to enhance the beauty of nature and boost the economy associated with the coastline (fishing and tourism) which accounts for 40% of the country’s gross domestic product (Nayananda 2007). Such an important coastal zone can be destroyed due to many reasons, including shoreline erosion, hazardous storms, and anthropogenic events. Shoreline change detection provides scientific methods and solutions to protect and develop the coastal zones in Sri Lanka. The shoreline position changes in Sri Lankan coastal zones are mainly controlled by the monsoon seasonality (Amalan et al. 2018; Gunasinghe et al. 2021; Ratnayake et al. 2018, 2019). For example, four monsoon seasons such as the southwest monsoon

from May to September, northeast monsoon from December to February, first inter-monsoon from March to April, and second inter-monsoon from October to November dominate the climate in Sri Lanka. According to the literature, cyclones are rare south of 10° N latitude in the Indian Ocean, but a few occurrences of extreme cyclone storms were recorded along the east coast of Sri Lanka such as the Rameswaram cyclone in December 1964 (Chittibabu et al. 2002; Srisangeerthan 2015). During the study period, no storms were reported near the west coast of Sri Lanka. The long term (period of 11 years, from 2006 to 2017) sea-level variation rate at the west coast of Sri Lanka is  $0.288 \pm 0.118$  mm/month (Palamakumbure et al. 2020). Accordingly, the average sea-level variation on the west coast of Sri Lanka from 2015 to 2021 was 12 mm. Therefore, shoreline position variations due to sea-level changes in the study area with a 10–15° beach slope are negligible and fall within the error margin of shoreline measurement of the current study. Furthermore, Sri Lanka is located in the middle of the geologically and tectonically stable Indo-Australian plate (Cooray 1984; Weththasinghe et al. 2021), and uplift, downwarping, and subsidence are negligible in the study locations.

The main purposes of this study are to (1) detect shoreline changes using ‘CoastSat’ software which is an open-source and python-based program (Vos et al. 2019a), (2) describe the coastal geomorphology, and (3) provide scientific information for coastal resource management practices for decision-making purposes to maintain a proper coastal management system along the west coast of Sri Lanka.

## 2 Study Area

The coastal environment of Sri Lanka focused on this study (Mount Lavinia, Agulana-Ratmalana, and Kalutara located on the west coast) is wave-dominated (average significant wave height of 1.12 m) and micro-tidal (mean tidal range of 0.7 m) (Duong et al. 2017; Ratnayake et al. 2013). The beaches are comprised of quartz sand with average grain diameters ( $D_{50}$ ) between 0.20 and 0.25 mm along the west coast of Sri Lanka (Ratnayake et al. 2019). Mount Lavinia Beach, one of the famous tourist destinations in the country, is located about 14 km south of Colombo, the commercial capital city of Sri Lanka (Fig. 1). The average beach width of Mount Lavinia is 30 m (Ratnayake et al. 2018) and the average beach length is 4 km including a headland that affects natural sediment transport processes. Agulana-Ratmalana Beach is located about 16 km south of Colombo, and it is also an important location for tourism (Fig. 1). The average beach width and length of Agulana-Ratmalana are approximately 20 m and 2 km, respectively (Ratnayake et al. 2018). Kalutara Beach (also known as

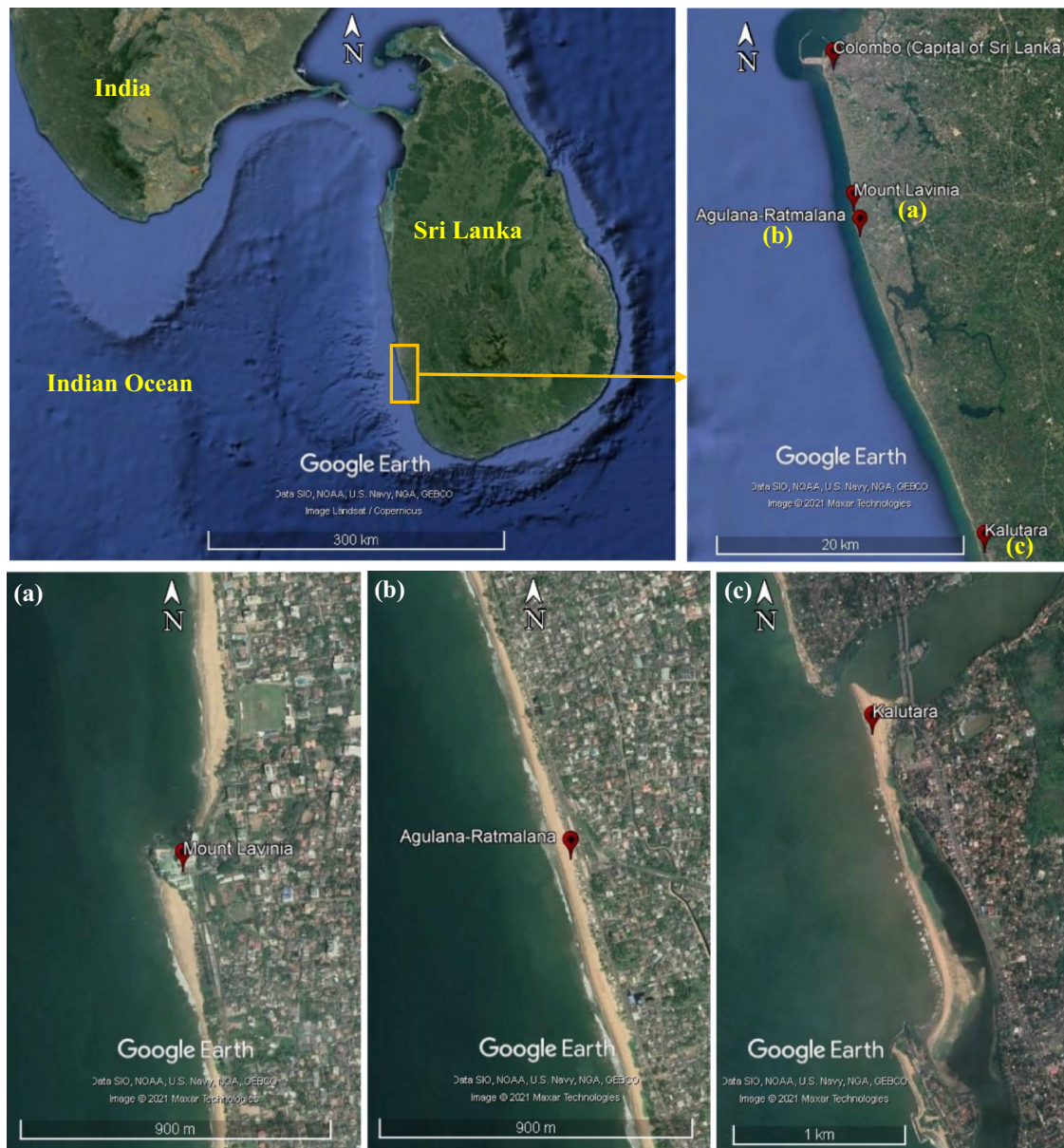


**Fig. 1** Location map of Mount Lavinia, Agulana-Ratmalana, and Kalutara beach study sites in West coast of Sri Lanka

Calido Beach) is located about 43 km south of Colombo (Fig. 1). The average beach width and length of Kalutara are approximately 22 m and 5 km, respectively, including Kalu Ganga (River) estuary, river outlet, and sand spit bar featuring complex geomorphology (Gunasinghe et al. 2021).

**2.1 Regional Settings**

During the last decade, the following significant coastal events have influenced changes in the coastline of the west coast of Sri Lanka.

- (1) The expansion of the construction industry since 2010 has caused the reduction in sand supply to beaches due to an increase in river sand mining.
- (2) The expansion of Colombo South Harbor, the establishment of a sand nourished port city, and the construction of a 5 km-long breakwater have altered sediment transport patterns along the western coast of Sri Lanka (Ratnayake et al. 2018).
- (3) A major sand spit bar (1.5 km long) was demolished at Kalu Ganga (River) mouth due to poor flood controlling measures in May 2017.
- (4) A sand nourishment program was carried out in the first quarter of 2020 on the west coast (Mount Lavinia,

Agulana-Ratmalana, and Kalutara) by the Coast Conservation and Coastal Resource Management Department (CC and CRMD) of Sri Lanka.

Many locations on the west coast of Sri Lanka suffer from severe erosion, which has created several coastal-related issues such as loss of beaches for tourism and recreational activities, increased difficulty in mooring fishing boats, and increased risk to dwellings located on the coastal belt. As an initial step in addressing such issues, shoreline change detection can be used to execute an appropriate coastal management system.

### 3 Methodology

Based on the most dynamic and widely used shorelines on the west coast of Sri Lanka, three beaches, namely, Mount Lavinia (ML), Agulana-Ratmalana (AR), and Kalutara (KL), were selected for this study (Fig. 1).

#### 3.1 Change Detection of Shorelines

The open-source software ‘CoastSat’ toolkit was used to extract shoreline positions pertaining to the study areas (Mount Lavinia, Agulana-Ratmalana, and Kalutara) in the present analysis. The ‘CoastSat’ is a Python-based program that is capable of acquiring time-series of shoreline positions (with a horizontal accuracy  $\sim 10$  m) in any coastal zones in the world using publicly available satellite images that have been archived in Google Earth Engine (GEE) for more than 30 years (Vos et al. 2019a, b). To obtain shoreline positions in the coastal zones from the ‘CoastSat’ software, the Landsat-5, Landsat-7, Landsat-8, and Sentinel-2 satellite images can be used, and these images are archived in the GEE (Table 1). The Sentinel-2 satellite images, which have 10 m spatial resolution in Red, Green, Blue, Near Infra-Red (NIR) bands and 20 m spatial resolution in Short Wave Infra-Red 1 (SWIR1) band, have been available from 2015 and were appraised for this study. Compared with the spatial resolution of Landsat images (30 m), Sentinel-2 images have improved spatial resolution and are the most suitable for shoreline detection and extraction.

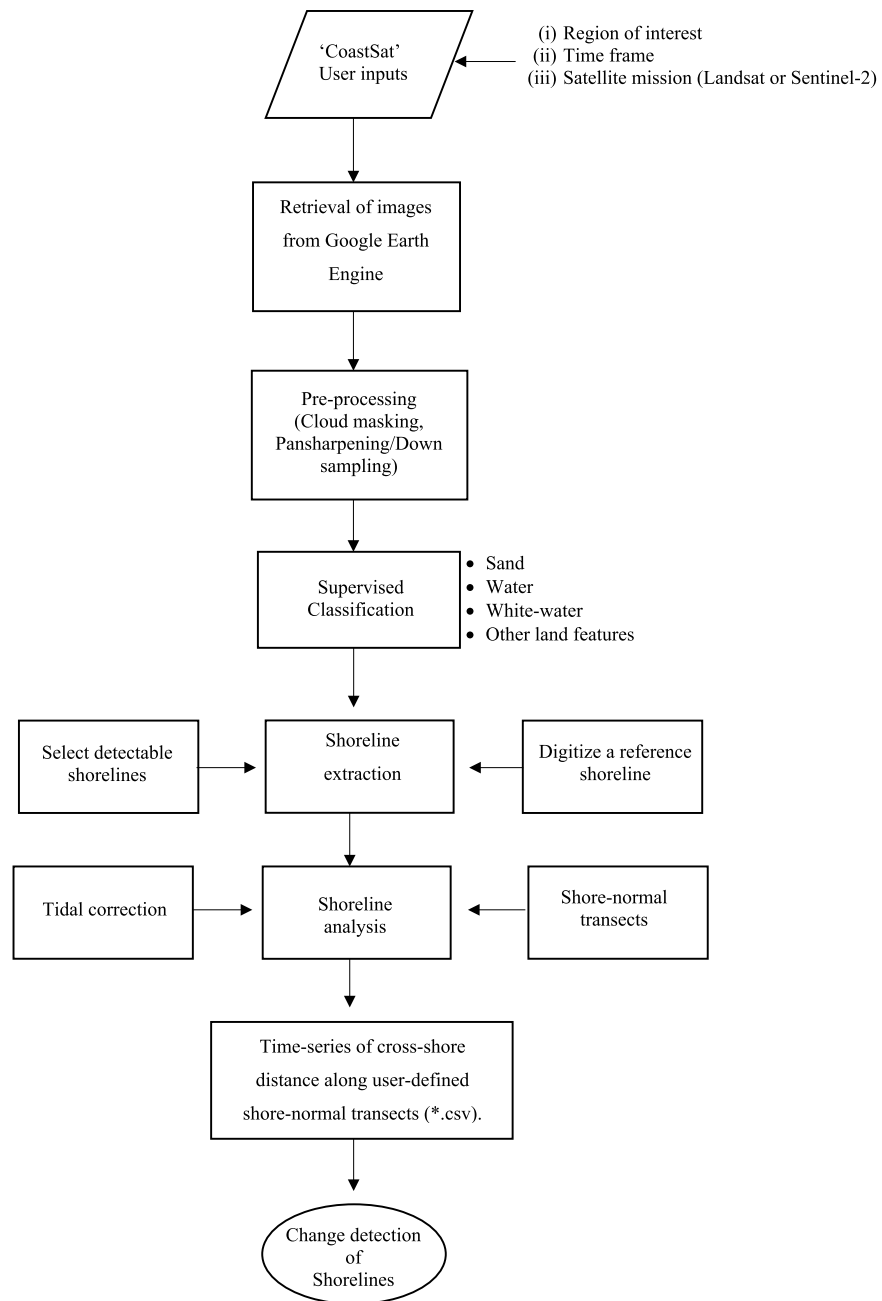
Traditional, medium spatial resolution satellite images, such as Landsat-8 with 30 m spatial resolution, are powerful enough for mapping regional-scale landscape elements (Amaro et al. 2015; Goncalves and Awange 2017; Parrish et al. 2005; Saleem and Awange 2019; Yu et al. 2011). Furthermore, it is possible to obtain more accurate coastline information to improve the understanding of shoreline changes with the use of European Sentinel-2 satellite data with higher temporal (5 days) and spatial (10 m) resolution (Immitzer et al. 2018; Saleem and Awange 2019; Topouzelis et al. 2016; Yang and Li 2012). Based on the published results of the analysis of shoreline changes using Sentinel-2 satellite images carried out during 2015–2020 elsewhere, it was found that the average shoreline changes are comparable with actual field-based measurements (Astiti et al. 2019; Cabezas-Rabadán et al. 2019; Mitri et al. 2020; Saleem and Awange 2019).

Figure 2 represents the flowchart of the different steps involved in obtaining a satellite-derived shoreline on a user-defined region of interest (ROI). Initially, the user can insert the information into the ‘CoastSat’, such as region of interest, dates (starting date and end date to retrieve satellite images), and satellite mission (Landsat and/or Sentinel-2). After that, users can retrieve and download a time-series of satellite images from GEE with the metadata. The downloaded images were pre-processed to remove cloud pixels and improve spatial resolution using cloud masking, and panchromatic image sharpening and down-sampling methods, respectively, before the shoreline positions were extracted. These pre-processed images were classified into four spatial classes such as sand, water, white-water, and other land features using the supervised classification method. Furthermore, sub-pixel resolution border segmentation was executed to extract the boundary between sand and water (the instantaneous shoreline) using the Modified Normalized Difference Water Index (MNDWI) that was applied to each classified image. Furthermore, one of the cloud-free, pre-processed, and classified images was then utilized to define the reference shoreline (the user has the option to manually digitize the reference shoreline in ‘CoastSat’, and coordinates of this reference shoreline provide a reference to subsequent shoreline demarcation and help to identify outliers and false detection) before the shoreline detection in

**Table 1** Metadata of the satellite images that are involved in ‘CoastSat’. Source: (Vos et al. 2019a)

Satellite mission	Time coverage	Revisit period	Pixel size
Landsat-5 (TM)	1984–2013	16 days	30 m R, G, B, NIR, SWIR1 bands
Landsat-7 (ETM+)	1999–present	16 days	30 m R, G, B, NIR, SWIR1 bands and 15 m panchromatic band
Landsat-8 (OLI)	2013–present	16 days	30 m R, G, B, NIR, SWIR1 bands and 15 m panchromatic band
Sentinel-2 (MSI)	2015–present	05 days	10 m R, G, B, NIR and 20 m SWIR1

**Fig. 2** Flow chart of the shoreline position extraction from ‘CoastSat’ toolkit



the ROI was commenced. The shore-normal transects were defined on the extracted shorelines to determine the time-series of cross-shore distance (obtained as a \*.csv).

Tidal correction was applied to all extracted shorelines using time-series of water-level data downloaded from the University of Hawaii Sea Level Center (<http://www.ioc-sealevelmonitoring.org/map.php>). The sand–water boundary of the classified satellite image extracted at a specific tidal stage is considered as the instantaneous shoreline position (Vos et al. 2019a). Although the instantaneous shoreline position would not be suitable for inter-comparison of shorelines, it is extracted by different stages of tide. Therefore, the

instantaneous shoreline positions (different stage of tides) extracted by classified satellite images should be projected to the single reference tidal datum to enable the inter-comparison. Accordingly, mean sea level (MSL) is utilized as the tidal reference datum of this study. According to Vos et al. (2019a), there is an equation to obtain MSL based shoreline positions as follows:

$$\Delta x = \frac{z_{ref} - z_{tide}}{m},$$

where  $\Delta x$  is the cross-shore horizontal shift (along the transect),  $z_{ref}$  is the reference tidal datum,  $z_{tide}$  is the

measured (or modeled) water level at the time of image acquisition, and  $m$  is the beach face slope specific to the site of interest. In this study,  $z_{\text{ref}}$  is considered as zero because tidal reference datum is mean sea level. Furthermore,  $m$  is 0.1 at each site (Mount Lavinia, Agulana-Ratmalana, and Kalutara) that was obtained from already published work (Gunasinghe et al. 2021; Ratnayake et al. 2018) using total station surveys and Global Navigation Satellite System surveys. The ‘CoastSat’ toolkit is required to insert correct parameters of  $z_{\text{ref}}$ ,  $z_{\text{tide}}$ ,  $m$  and capable of calculating the MSL based shoreline positions. More information concerning tidal correction and ‘CoastSat’ is available in (Vos et al. 2019a).

In Mount Lavinia, Agulana-Ratmalana, and Kalutara, WGS 84 coordinates of ROI (polygon) covering a 1 km-long coastline in each study area were entered in the ‘CoastSat’ software. The satellite mission was inserted as ‘S2’ (Sentinel-2), and the satellite image acquisition time length was expanded from 1 January 2015 to 1 April 2021 for each location. In addition, the ‘CoastSat’ program was executed for each study area separately. The ‘CoastSat’ retrieved 266 images (Sentinel-2 with a spatial resolution of 10 m, the horizontal accuracy of ‘CoastSat’  $\sim 10$  m) each for Mount Lavinia and Agulana-Ratmalana, and 265 images (Sentinel-2 with a spatial resolution of 10 m, the horizontal accuracy of ‘CoastSat’  $\sim 10$  m) for Kalutara. Furthermore, 51, 56, and 49 images were selected for shoreline analysis in Mount Lavinia, Agulana-Ratmalana, and Kalutara, respectively, after the pre-processing and classification process. The time gap between selected images was approximately 30 days. Furthermore, the constant time gap between images used to extract shoreline positions is important to analyze shoreline changes in each location. The four shore-normal transects were defined by approximately equal distance in each location (Fig. 3) within a 1 km-long coastline. After applying tidal corrections to the extracted shorelines at each location, the time-series of cross-shore distances along shore-normal transects (from landward to seaward) were determined, and resultant data files were obtained as an MS-Excel \*.csv format from the ‘CoastSat’ and, eventually, the time-series of shoreline change along each transect was plotted on a graph using the resultant data file MS-Excel \*.csv.

The accuracy of shoreline position extracted by ‘CoastSat’ was verified by comparing it with the shoreline field survey data obtained through the Global Navigation Satellite System (GNSS) technology (TOPCON GR5 GNSS receiver) along with Sri Lanka Continuously Operating Reference Station Network (SLCORSnet) correction (horizontal accuracy—0.007 m). Accordingly, the average difference between shoreline position obtained from ‘CoastSat’ and the field survey was calculated in two locations: (1) Agulana-Ratmalana and (2) Kalutara. However, measured field data

of past shorelines were not available in Mount Lavinia for accurate assessment of shorelines extracted from ‘CoastSat’.

### 3.2 Overall Beach State

The overall beach state (Table 2) within the time frame that was considered to extract shorelines in this study was determined by calculating the distance between the preceding and succeeding shorelines in each shore-normal transects of respective locations.

### 3.3 Seasonal Longshore Current Direction

The seasonal longshore current directions in study locations (Mount Lavinia, Agulana-Ratmalana, and Kalutara) of this investigation were obtained from published results in scientific journals (Table 3).

## 4 Results and Discussion

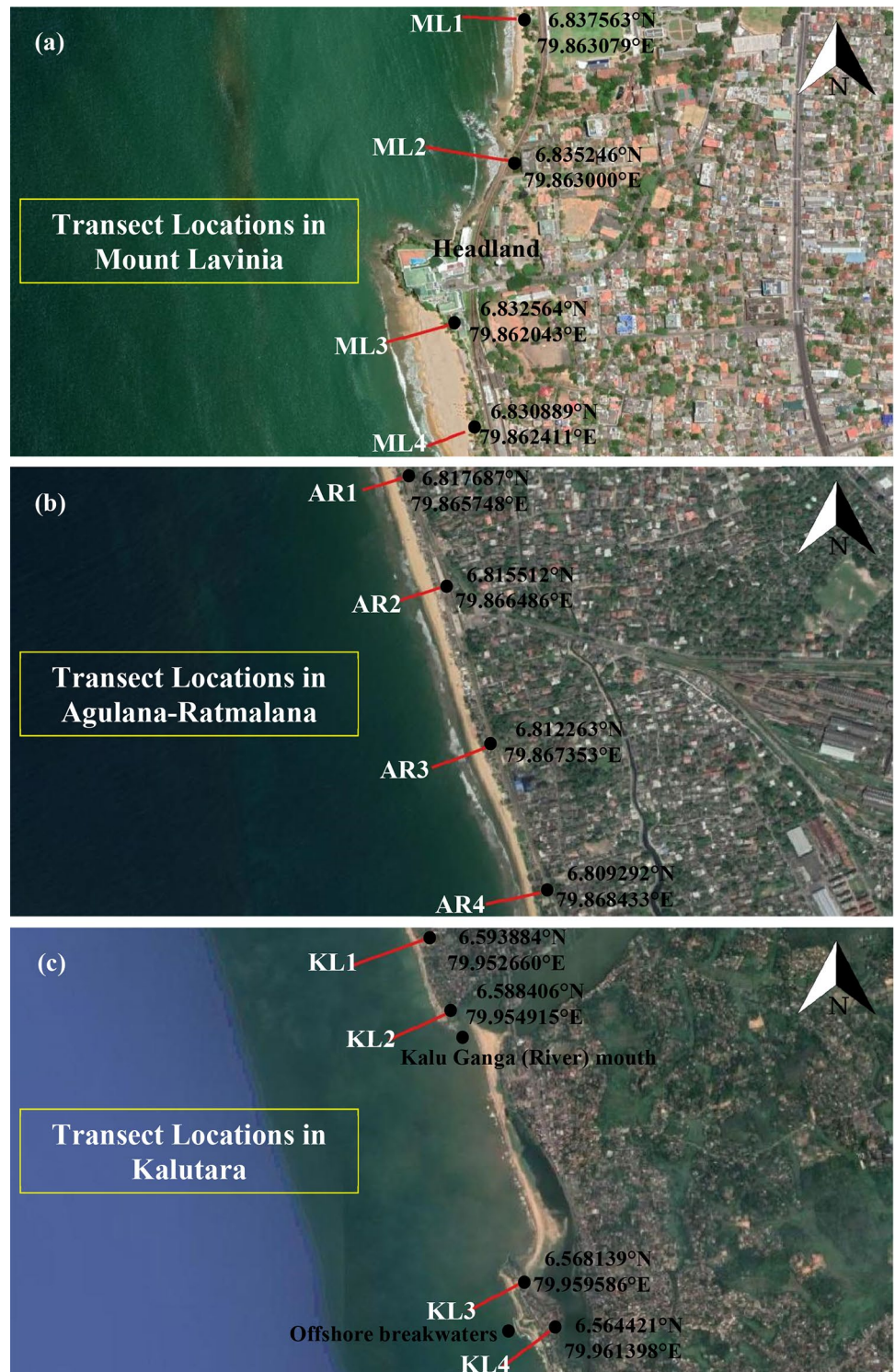
### 4.1 Horizontal Difference of Shoreline Position (‘CoastSat’ and Field Observations)

The average horizontal difference between shoreline positions extracted by ‘CoastSat’ and field observations was  $7.5 \pm 1$  m in Agulana-Ratmalana on 19 August 2019 and was  $8.3 \pm 1$  m in Kalutara on 29 July 2020 (Fig. 4). In addition, the obtained error margin (7–8 m) was less than the horizontal accuracy of coastline positions of ‘CoastSat’ ( $\sim 10$  m). Therefore, it is suggested that the horizontal difference of shoreline positions (‘CoastSat’ and field observations) is within an acceptable range.

### 4.2 Seasonal Geomorphological Changes in Mount Lavinia

Figure 5a illustrates 51 shore-normal distances along each transect for the image acquisition date. Accordingly, most of the sand accretion in each transect was represented during the northeast monsoon and inter-monsoon seasons (26 April 2016, 10 February 2017, 18 October 2018, and 01 January 2020). However, most of the sand erosion was represented during the southwest monsoon season (29 August 2017, 08 September 2018, 25 July 2019, and 29 July 2020). Furthermore, the overall beach state during the study period (from 2016 to 2021) in the ML1 and ML2 transects shows sand accretion, while other ML3 and ML4 transects show sand erosion (Table 2). The largest erosion and accretion values are 17 m along ML3, and 27 m along ML1, respectively. Furthermore, mean values and standard deviations of each transect are given in Table 2.

**Fig. 3** Locations of transects in study area (transect coordinates are decimal degrees with respect to WGS 84 datum), **a** Mount Lavinia, **b** Agulana-Ratmalana, **c** Kalutara (transects are not into a scale)



Accordingly, the overall accretion and erosion were 22.5 m in the North of the headland and 14.5 m in the South of the headland, respectively. Furthermore, the significant changes of shoreline position in transect ML1 starting from 16 March 2020 and 23 August 2020 were gradual accretion and erosion, respectively. Similarly, in transect ML2, rapid

accretion and erosion can be seen from 16 March 2020 and 20 April 2020, respectively. Furthermore, the rapid erosion was obvious along the transect ML3 during the period of 10 May 2020 to 29 July 2020 in the southwest monsoon season. In addition, there were no significant changes along the transect ML4 during the study period.

**Table 2** Overall beach state, gain and loss, mean, and standard deviation in Mount Lavinia, Agulana-Ratmalana, and Kalutara

Location	Transect	Number of shorelines extracted	Time frame	Distance between proceeding (OL) and succeeding (YG) shorelines (OL-YG) m		Overall beach state	Mean (m)	Standard deviation
				Gain	Loss			
Mount Lavinia	ML1	51	2016–2021	27		Accretion	36.42	16.64
	ML2	51	2016–2021	18		Accretion	35.92	22.46
	ML3	51	2016–2021		17	Erosion	57.61	18.12
	ML4	51	2016–2021		12	Erosion	39.56	09.81
Agulana-Ratmalana	AR1	56	2016–2021	03		Steady state	40.52	12.61
	AR2	56	2016–2021	22		Accretion	44.98	13.27
	AR3	56	2016–2021	30		Accretion	40.36	16.34
	AR4	56	2016–2021	25		Accretion	42.99	18.08
Kalutara	KL1	49	2016–2021	01		Steady state	112.62	14.33
	KL2	49	2016–2021		56	Erosion	99.42	20.30
	KL3	49	2016–2021	20		Accretion	85.67	08.84
	KL4	49	2016–2021		01	Steady state	99.64	07.07

**Table 3** The investigations about the wave directions and longshore current directions based on the monsoon seasonality along the West coast of Sri Lanka

Location of the study	Time period of the study	Predominant longshore current direction				Source
		Southwest monsoon	Northeast monsoon	1st inter-monsoon	2nd inter-monsoon	
West Coast	1968–1986	Northward	Southward	Negligible	Negligible	Chandramohan et al. (1990)
Wadduwa (West Coast)	2014–2016	Northward	Southward	Not available	Not available	Amalan et al. (2018)
Uswetakeiyawa (West Coast)	2014–2015	Northward	Southward	Northward	Northward	Ratnayake et al. (2019)
Kalutara (West Coast)	2017	Northward	Southward	Northward	Northward	Gunasinghe et al. (2021)

The shoreline changes depend on many factors such as the existing shape of the shoreline, source and sink of sediment, strong storms, and hydro-sedimentary dynamics (Amalan et al. 2018; Anfuso et al. 2020; Deepika et al. 2014; Flor-Blanco et al. 2021; Guisado-Pintado and Jackson 2018; Gunasinghe et al. 2021; Harris et al. 2020; Héquette et al. 2019; Ratnayake et al. 2018, 2019; Yang and Dong 2017). Furthermore, the longshore currents along with cross-shore transport govern the erosion/accretion pattern of beaches due to storm and calm weather conditions generated with monsoonal changes (Gunasinghe et al. 2021; Rajith et al. 2008; Ratnayake et al. 2018, 2019).

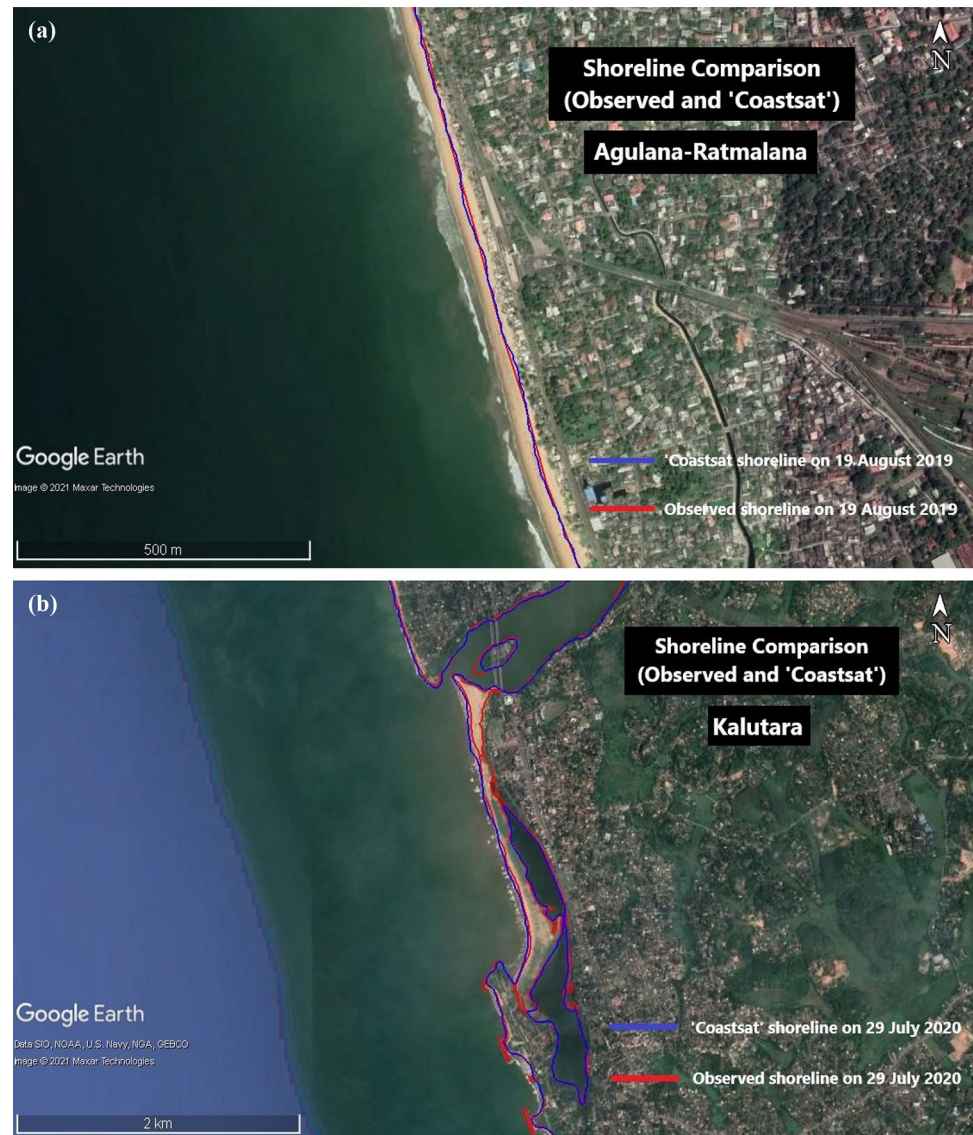
In Mount Lavinia, the significant wave heights during the northeast and inter-monsoon seasons are comparatively low due to the calm wave climate (Amalan et al. 2018; Chandramohan et al. 1990; Gunasinghe et al. 2021; Ratnayake et al. 2019). Therefore, most of the offshore sands are transported shoreward with energetic waves with long periods

generated by onshore currents, and accretion was noticeable in the area. In addition, the significant wave height during the southwest monsoon was comparatively high due to the energetic wave conditions (Amalan et al. 2018; Chandramohan et al. 1990; Gunasinghe et al. 2021; Ratnayake et al. 2019). Due to the strong backwash generated by the offshore currents, most of the beach sand is transported offshore causing erosion during the southwest monsoon. The same process was observed by many researchers through field investigation programs on the west coast of Sri Lanka (e.g., Miles and Russell 2004; Ratnayake et al. 2018, 2019; Ruggiero et al. 2001; Zhang et al. 2004).

A sand nourishment program was initiated in the study area during the first quarter of 2020 by the Coast Conservation and Coastal Resource Management Department (CC and CRMD), Sri Lanka. Due to sand nourishment in the North of the headland (around ML2), the accretion was apparent from 16 March 2020 (Fig. 5a). During



**Fig. 4** Shoreline comparison between 'CoastSat' and field measurements, **a** Agulana-Ratmalana (AL), **b** Kalutara (KL)



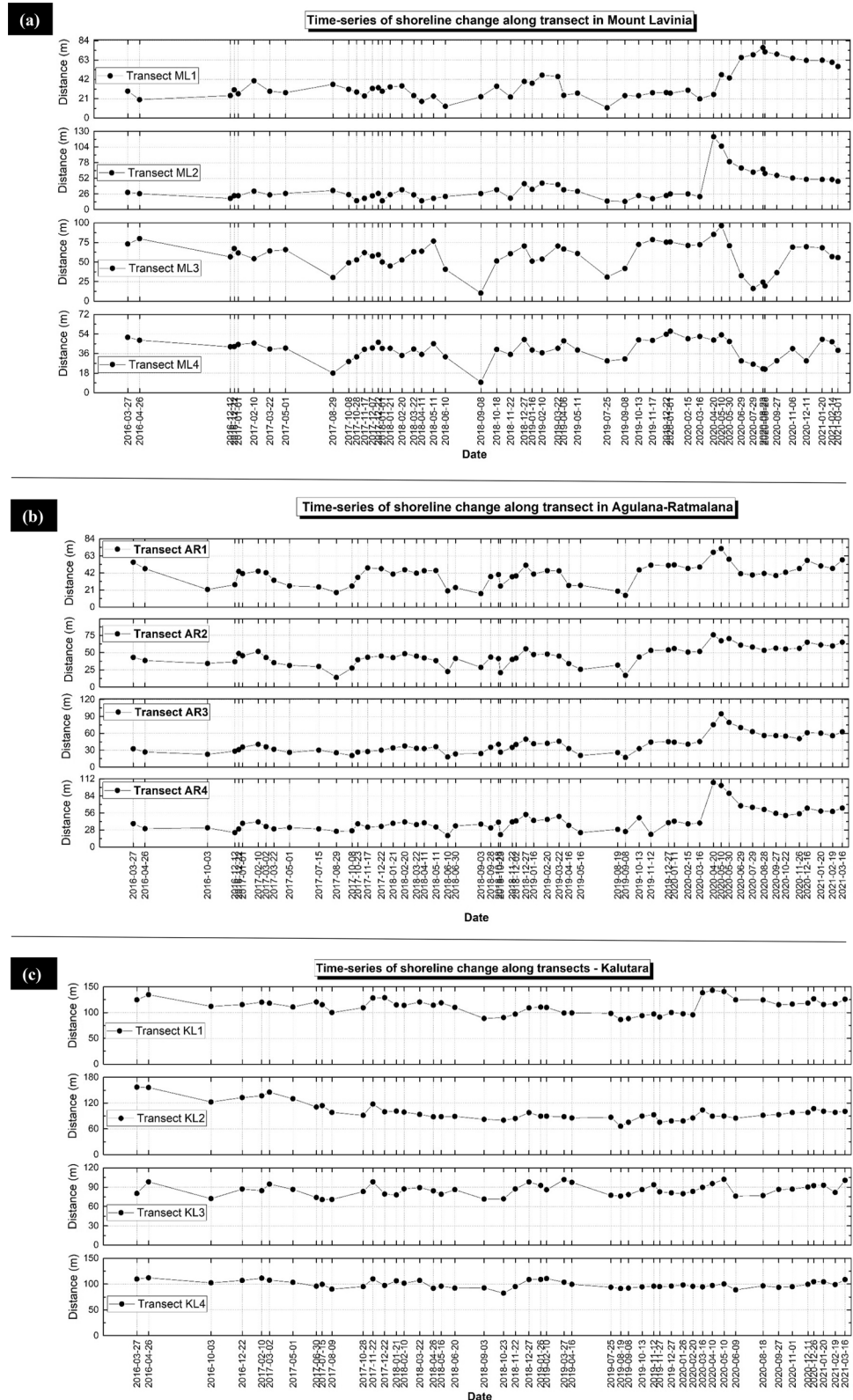
this period, the 1st inter-monsoon season commenced, and consequently, the longshore current direction was heading towards the north (Table 3) with calm wave conditions (Amalan et al. 2018; Chandramohan et al. 1990; Gunasinghe et al. 2021; Ratnayake et al. 2019). Accordingly, some of the nourished sand in the North of the headland moved in a northerly direction along the shoreline. Furthermore, the process was accelerated with the onset of the southwest monsoon due to the energetic wave climate. Therefore, rapid erosion was observed in and around ML2 from 20 April 2020. In addition to the longshore currents, cross-shore sediment transport also eroded the nourished beach with strong offshore currents during the southwest monsoon. Part of this offshore sand was transported back onshore with the onset of calm northeast monsoon weather. Even though high-resolution satellite images are not available to visualize the process, still photographs

taken soon after the sand nourishment clearly show the difference (Fig. 6).

The erosion was evident in and around ML1 from 23 August 2020 (Fig. 5a). Furthermore, erosion in and around ML2 was more rapid than in and around ML1 due to obstruction of northward sand transport processes because of the headland. The erosion process was slow in and around ML1 due to the sand transport from ML2 to ML1 by longshore currents.

The longshore drift during the southwest monsoon is towards the North along Mount Lavinia Beach (Table 3). Furthermore, the headland that is shown in Fig. 3a traps the sand which is moving towards the North resulting in sand accumulation in the south of the headland (Fig. 7). Therefore, transects ML3 and ML4 represent sand accretion during the southwest as well as northeast monsoons. In addition, the wavefronts that approached from the southwest direction

**Fig. 5** Time-series of shoreline change along each transects, **a** Mount Lavinia (ML), **b** Agulana-Ratmalana (AR), **c** Kalutara (KL)



to the beach during the southwest monsoon (Amalan et al. 2018; Chandramohan et al. 1990; Gunasinghe et al. 2021; Ratnayake et al. 2019) were refracted near the headland.

The refracted wavefronts were propagated parallel to the beach in the North of the headland, reducing longshore drift and producing a steady-state beach condition (Fig. 7).

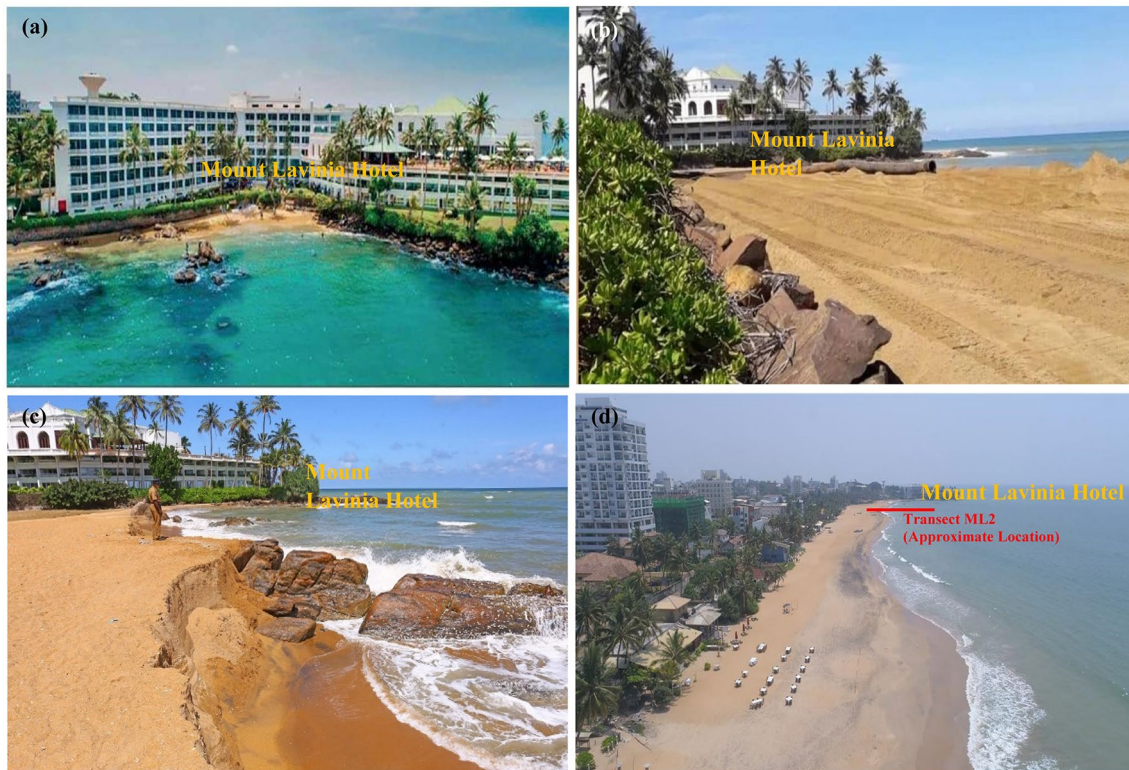


**Fig. 6** The Mount Lavinia beach, **a** before the sand nourishment project (DailyFT 2020), **b** soon after the sand nourishment project (Chandrasekharthi 2020), **c** after the beach erosion due to monsoon effects (Jayathillake 2020), **d** present situation of the beach (Dailymirror 2021)

After the beach nourishment program, this beach area in Mount Lavinia has become erosional, since wavefronts are approaching angular to the beach. Consequently, most of the sand was eroded and transported offshore due to the high-energy breaking waves with small wave periods generated offshore currents during the first inter-monsoon and after southwest monsoon season. Furthermore, some sand was transported to the North due to the longshore currents. The nourished sand to the North of the headland was thus washed out quickly. The same observation was discussed and evidenced by Pattiaratchi et al. (2020).

### 4.3 Seasonal Geomorphological Changes in Agulana-Ratmalana

According to Fig. 5b, 56 shore-normal distances (along each transect) are plotted for the image acquisition date. The accretion and erosion were obvious during the northeast and inter-monsoon seasons (27 March 2016, 10 February 2017, 18 October 2018, and 27 December 2019), and southwest monsoon season (01 May 2017, 10 June 2018, 16 May 2019, and 28 August 2020), respectively. Furthermore, the overall beach state along most of the transects at AR1, AR2, and AR3 shows accretion, whereas there was a steady-state

condition at AR4 during the study period (Table 2). The largest accretion value is 30 m along AR3. Furthermore, mean values and standard deviations of each transect are available in Table 2. In addition, significant accretion and gradual erosion can be seen in each transect from 16 March 2020 and 10 May 2020, respectively. The sand accretion was evidenced due to the implemented sand nourishment program in the study area in the 1st quarter of 2020 and gradual erosion occurred due to the longshore currents and cross-shore currents based on monsoon seasonality.

The accretion and erosion occurred due to normal wave conditions along with seasonal monsoon changes in the study area as described in seasonal geomorphological changes in Mount Lavinia. The 1st inter-monsoon season began from March 2020 and waves came from a southward direction during this period (Amalan et al. 2018; Chandramohan et al. 1990; Gunasinghe et al. 2021; Ratnayake et al. 2019). Consequently, the longshore drift was directed towards the North (Table 3), supplying sand to the beaches. A few months later, with the onset of the southwest monsoon season in the area, the process of transporting sand to the North intensified compared to the previous inter-monsoon season. This process is represented from the transect-based shoreline changes in Fig. 5b. Moreover,



**Fig. 7** Present nearshore coastal dynamics at Mount Lavinia beach during the dominant southwest monsoon

after the 2nd inter-monsoon and northeast monsoon seasons, gradual accretion was evident due to high-energy wave action with long-period waves generated onshore transport under calm weather. In this period, waves approached from the southwest direction and wavefronts were parallel to the beach (based on the orientation and shape of the beach). Subsequently, onshore and offshore sediment transport rates controlled the accretion/erosion processes in this location (Fig. 8).

From 2016 to the end of 2019, the shoreline changes of all transects in the study area represent gradual coastal erosion. The reasons for this change are: (1) the orientation and (2) the shape of the shoreline in Agulana-Ratmalana. The orientation and shape of the shoreline in this location are found as directed towards the northwest and a straight shoreline, respectively. The waves arrive perpendicular to the beach during the southwest monsoon, and thus, erosion is mainly due to the cross-shore currents (Fig. 8). Consequently, only a gradual erosion is evident in this location during both southwest monsoon and northeast monsoon seasons.

Ratnayake et al. (2018) also reported that the construction of a 5 km-long breakwater in the Colombo Harbor

Expansion Project alters sediment transport patterns along the western coast of Sri Lanka. It is thought that most of the sand was trapped by this breakwater. Sand supply to the beaches in the South with the southerly longshore currents occurring during the northeastern monsoon is considerably less. Therefore, the erosion process was evident in many places on the west coast as shown in the transects AR1, AR2, AR3, and AR4.

#### 4.4 Seasonal Geomorphological Changes in Kalutara

The 49 shore-normal distances (along each transect) for the image acquisition date were plotted during the study period (Fig. 5c). As mentioned in previous study locations, both accretion and erosion were obvious during the northeast and inter-monsoon seasons (26 April 2016, 02 March 2017, 27 December 2017, and 27 December 2019), and southwest monsoon season (30 June 2017, 09 August 2017, 03 September 2018, and 19 August 2019), respectively. Furthermore, the overall beach state derived from transect-based shoreline distances during the study period (from 2016 to 2021) shows sand accretion along



**Fig. 8** Present nearshore coastal dynamics at Agulana-Ratmalana beach during the dominant southwest monsoon

the transects KL1 and KL3 and sand erosion along the transects KL2 and KL4 (Table 2). The largest erosion and accretion values are 56 m along KL2 and 20 m along KL3, respectively. Mean values and standard deviations of each transect are available in Table 2. Moreover, the shorelines belonging to transect KL3 and KL4 located in Kalutara South indicate smaller changes compared with shorelines belonging to transect KL1 and KL2 located in Kalutara North, which lead to stable beach conditions.

The wave climate due to the seasonal monsoons controls the beach accretion and erosion in the study area as described in seasonal geomorphological changes in Mount Lavinia. Rapid accretion was seen in transect KL1 from 20 February 2020 due to the sand nourishment program in this area. The nourished sand is then gradually eroded and moved northward due to longshore currents (Table 3). The shoreline in and around KL1 was eroded relatively rapidly from 18 August 2020 due to the severe cross-shore and longshore sediment transport during the southwest monsoon season. The accretion in and around KL2 (it was low

compared with KL1) started on 20 February 2020 due to the sand nourishment program in Kalutara North.

The shoreline around KL2 was gradually eroded from 2016, and it was significant from 30 May 2017. In May 2017, a considerable part of the sand spit bar (also known as Calido Beach) was demolished to control floods in the study area. As a result, severe coastal erosion has taken place (Gunasinghe et al. 2021). Furthermore, transect KL2 is located very close to the newly formed river mouth of Kalu Ganga (River), and a considerable amount of beach erosion has taken place during the southwest monsoons (Fig. 9) due to offshore transport with high-energy waves. Furthermore, the longshore drift is interrupted at the river mouth, thus trapping sand (Fitzgerald 1988; Hayes 1991; Oertel 1988), which reduces the sand supply to the northern beaches of Kalutara, further eroding the KL2 transect area. In summary, the main causes for the significant erosion in the Kalutara area are as follows: (1) interruption of longshore drift at the river mouth, (2) reduced sand supply from the north of Kalutara, and (3) formation of a new river mouth after the demolition of the sand spit bar at Calido Beach.

In the shoreline of transect KL3 and KL4, during the southwest monsoon, beaches were eroded due to the high wave energy action, and during the northeast monsoon, beaches were re-developed due to the calm wave conditions. Therefore, the southern beaches in Kalutara are in a stable condition due to the adoption of coastal conservation strategies by the construction of offshore breakwaters.

#### 4.5 Seasonal Longshore Current Direction

In general, waves approach the west coast in Sri Lanka from a southwest direction during the southwest monsoon season. Consequently, the longshore currents move towards the North along the coast. Furthermore, waves approach the west coast from a northwest direction during northeast monsoon season. The longshore currents move towards the South along the coast. The significant wave height in the southwest monsoon season was higher than that in the northeast monsoon seasons. In addition, significant wave height during the inter-monsoon season was lower than the southwest monsoon (Amalan et al. 2018; Chandramohan et al. 1990; Gunasinghe et al. 2021; Ratnayake et al. 2019).

The longshore current direction (Table 3) is determined by the wave direction for various monsoon seasons and coastal zone orientation to the wavefronts (Pinet 2019; Ratnayaka et al. 2018, 2019). Therefore, the longshore current direction is northward in each study location due to the waves approaching from the south, southwest, west–southwest, south–southwest, and northwest–southeast coastal zone orientation to the wavefronts (Fig. 10a). On the other hand, the longshore current direction is southward in each study location due to the waves coming from the north,

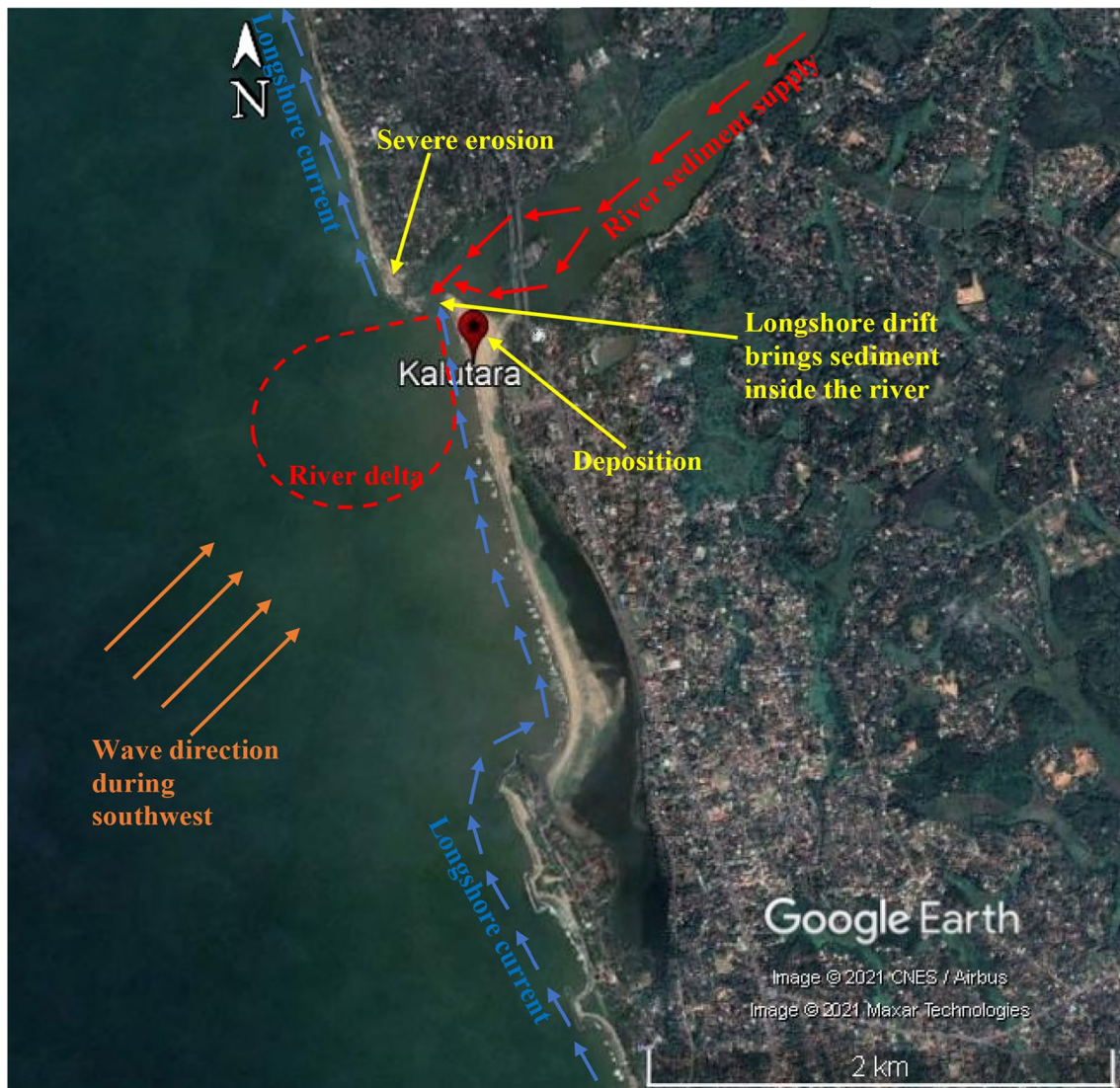


**Fig. 9** Present nearshore coastal dynamics at Kalutara beach during the dominant southwest monsoon

northwest, north–northwest, and west–northwest, while the studied coastal zone area is oriented in a northwest–southeast direction (Fig. 10b).

#### 4.6 Evaluation of Beach Nourishment Projects in Sri Lanka

Beach erosion is a serious problem on the west coast of Sri Lanka where most of the tourist hotspots are located. Maintaining steady-state beaches is important for the country's GDP (gross domestic products) growth. Hard engineering solutions may provide better solutions to beach erosion. However, being a tropical country with a significant tourism industry, wider sandy beaches are needed for recreational purposes. Therefore, sand nourishment is the better

soft engineering solution for controlling beach erosion and maintaining a steady beach state (Samarasekara et al. 2018).

Sri Lanka's first beach nourishment project was launched by the Coast Conservation Department in 2012 at Uswe-takeiyawa (10 km north of Colombo on the west coast of Sri Lanka), a 1.8 km coastal stretch. About 300,000 m<sup>3</sup> of offshore sand from the nearby offshore area was pumped off the coast using a dredging vessel. Ratnayake et al. (2019) collected beach profiles and sand samples from September 2014 to September 2015, and satellite imagery in the study area was analyzed between 2010 and 2015. This study indicated that the nourished beaches were severely eroded within a very short time. About 1 year after the beach was nourished, three breakwaters were constructed in the study area. However, the tombola structures or salient features were not properly developed in association with the breakwaters. The

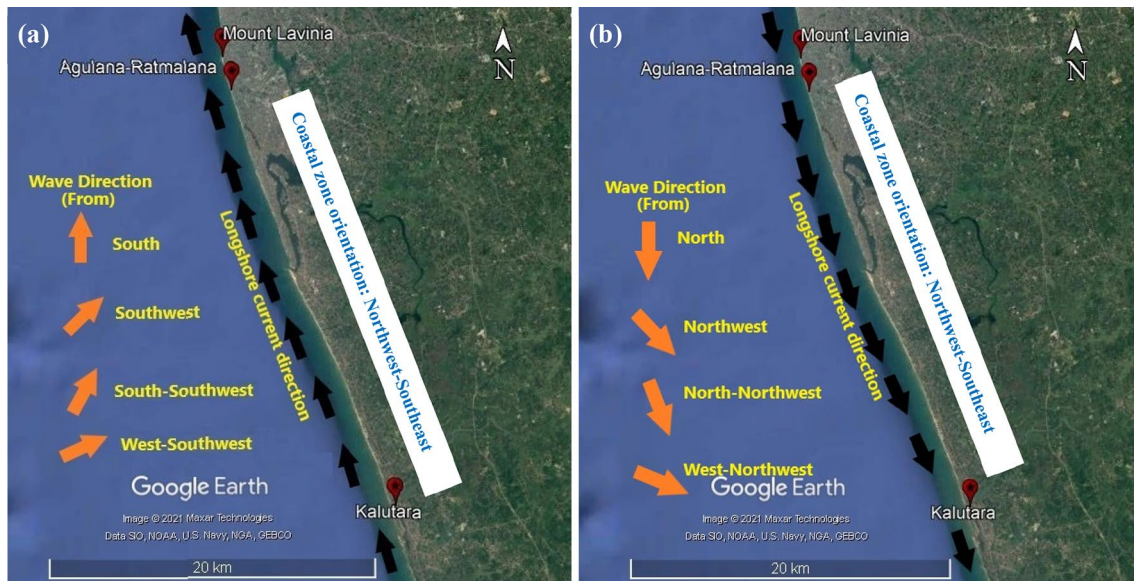


**Fig. 10** The longshore current directions based on the wave direction at the study area in the western coast of Sri Lanka, **a**) northward longshore current direction, **b** southward longshore current direction

grain size analysis from sand samples collected from the study area indicated the sand used for the beach nourishment is finer than native beach sand. It is generally accepted that the native beach sand in the study area should be approximately finer or equal to nourished sand. Therefore, the grain size of the nourished sand used in the project was partially inefficient. Furthermore, based on the field data collected, the breakwaters established to minimize sand erosion in the area have not been utilized (Ratnayake et al. 2019). The recent beach nourishment project in Mount Lavinia, Agulana-Ratmalana, and Kalutara areas has also not been a success as described in this study. However, future shoreline change studies in the overall area are necessary to access whether nourished sand was trapped within the coastal zone.

Experiences gained from the few beach nourishment projects in Sri Lanka demonstrate that a proper pre-feasibility study followed by a thorough environmental impact assessment (EIA) is vital before commencing any beach nourishment project. Therefore, extensive research on spatial and temporal shoreline detection similar to the present study is important to evaluate and implement successfully future beach nourishment projects in Sri Lanka.

## 5 Conclusion

The time-series of shoreline positions extracted from ‘CoastSat’ software (v1.1.1) were used for the detection of shoreline changes of three well-known beaches on the west coast of Sri Lanka: Mount Lavinia, Agulana-Ratmalana, and Kalutara. Furthermore, predominant longshore current direction

was utilized to examine coastal erosion and accretion processes. This study arrived at the following conclusions:

- (1) This study shows that the average difference of shoreline positions obtained by ‘CoastSat’ and field observation was 7–8 m.
- (2) When the long-term field measurements regarding coastal data are not available, an alternative method—CoastSat: A Google Earth Engine-enabled Python toolkit can be used to extract shoreline positions and the detection of coastline changes with appropriate tidal corrections. This method can be used in any coastal area in the world for shoreline change detection.
- (3) The overall beach state of the study area shows more than 10 m erosional and accretional trends based on monsoon seasonality and anthropogenic events.
- (4) Significant erosion was observed adjacent to the river mouth area of the Kalu Ganga (River) in the Kalutara coastline due to the breakage of the sand spit bar.
- (5) The natural longshore drift is interrupted by the natural headland during southwest and northeast monsoons, increasing coastal erosion in downdrift and increasing accretion in updrift in Mount Lavinia.
- (6) The coastal erosion is evident during the southwest monsoon due to the high-energy wave action (significant wave heights are high) in each study location.
- (7) The coastal accretion is evident during the northeast monsoon due to the calm wave conditions (significant wave heights are low) in each study location.
- (8) The shoreline change detection of this study reveals that the sand nourishment program initiated in the first

quarter of 2020 on the West coast of Sri Lanka has not influenced the change in beaches significantly in Mount Lavinia, Agurana-Ratmalan, and Kalutara.

**Acknowledgements** The authors gratefully acknowledge Dr. Nimal Wijeratne, Prof. Ranjith Premasiri, and anonymous reviewers for their valuable comments, and Ms. Ranjani Amarasinghe and Mr. Sadun Silva for their assistance in completing field activities related to this research project.

## References

- Ali PY, Narayana AC (2015) Short-term morphological and shoreline changes at Trinkat Island, Andaman and Nicobar, India, after the 2004 Tsunami. *Mar Geod* 38(1):26–39. <https://doi.org/10.1080/01490419.2014.908795>
- Alicandro M, Baiocchi V, Brigante R, Radicioni F (2019) Automatic shoreline detection from eight-band VHR satellite imagery. *J Mar Sci Eng* 7(12):459. <https://doi.org/10.3390/jmse7120459>
- Amalan K, Ratnayake AS, Ratnayake NP, Weththasinghe SM, Dushyantha N, Lakmali N, Premasiri R (2018) Influence of nearshore sediment dynamics on the distribution of heavy mineral placer deposits in Sri Lanka. *Environ Earth Sci* 77(21):1–13. <https://doi.org/10.1007/s12665-018-7914-4>
- Amaro VE, Gomes LRS, de Lima FGF, Scudelari AC, Neves CF, Busman DV, Santos ALS (2015) Multitemporal analysis of coastal erosion based on multisource satellite images, Ponta Negra Beach, Natal City, Northeastern Brazil. *Mar Geod* 38(1):1–25. <https://doi.org/10.1080/01490419.2014.904257>
- Anfuso G, Loureiro C, Taouati M, Smyth T, Jackson D (2020) Spatial variability of beach impact from post-tropical Cyclone Katia (2011) on Northern Ireland's North Coast. *Water* 12(5):1380. <https://doi.org/10.3390/w12051380>
- Astiti SPC, Osawa T, Nuarsa IW (2019) Identification of shoreline changes using sentinel 2 imagery data in Canggü Coastal Area. *Ecotrophic J Environ Sci* 13(2):191–204
- Boak EH, Turner IL (2005) shoreline definition and detection: a review. *J Coast Res* 21(4 (214)):688–703. <https://doi.org/10.2112/03-0071.1>
- Bouchahma M, Yan W (2012) Automatic measurement of shoreline change on Djerba Island of Tunisia. *Comput Inf Sci* 5(5):17. <https://doi.org/10.5539/cis.v5n5p17>
- Cabezas-Rabadán C, Pardo-Pascual JE, Palomar-Vázquez J, Fernández-Sarría A (2019) Characterizing beach changes using high-frequency sentinel-2 derived shorelines on the Valencian coast (Spanish Mediterranean). *Sci Total Environ* 691:216–231. <https://doi.org/10.1016/j.scitotenv.2019.07.084>
- Chand P, Acharya P (2010) Shoreline change and sea level rise along coast of Bhitarkanika Wildlife Sanctuary, Orissa: an analytical approach of remote sensing and statistical techniques. *Int J Geomat Geosci* 1(3):436
- Chandrakeerthi KP (2020) Another take on Mount Lavinia artificial beach project. <https://www.newsradio.lk/justin/another-take-on-mount-lavinia-artificial-beach-project/>. Accessed 07 May 2021
- Chandramohan P, Nayak BU, Raju VS (1990) Longshore-transport model for south Indian and Sri Lankan coasts. *J Waterw Port Coast Ocean Eng* 116(4):408–424. [https://doi.org/10.1061/\(ASCE\)0733-950X\(1990\)116:4\(408\)](https://doi.org/10.1061/(ASCE)0733-950X(1990)116:4(408))
- Chittibabu P, Dube SK, Sinha PC, Rao AD, Murty TS (2002) Numerical simulation of extreme sea levels for the Tamil Nadu (India) and Sri Lankan Coasts. *Mar Geod* 25(3):235–244. <https://doi.org/10.1080/01490410290051554>
- Cooray PG (1984) An introduction to the Geology of Sri Lanka. 2nd revised edition, Ceylon National Museum Publication, Colombo
- DailyFT (2020) Absence of EIA and wastage of public funds in Mt. Lavinia beach nourishment project. <http://www.ft.lk/Opinion-and-Issues/Absence-of-EIA-and-wastage-of-public-funds-in-Mt-Lavinia-beach-nourishment-project/14-701165>. Accessed 07 May 2021
- Dailymirror (2021) Artificial beach between Kalutara and Mount Lavinia is a success: Coast Conservation Department. [http://www.dailymirror.lk/breaking\\_news/Artificial-beach-between-Kalutara-and-Mount-Lavinia-is-a-success-Coast-Conservation-Dept/108-208486](http://www.dailymirror.lk/breaking_news/Artificial-beach-between-Kalutara-and-Mount-Lavinia-is-a-success-Coast-Conservation-Dept/108-208486). Accessed 07 May 2021
- Deepika B, Avinash K, Jayappa KS (2014) Shoreline change rate estimation and its forecast: remote sensing, geographical information system and statistics-based approach. *Int J Environ Sci Technol (tehran)* 11(2):395–416. <https://doi.org/10.1007/s13762-013-0196-1>
- Duong TM, Ranasinghe R, Luijendijk A, Walstra D, Roelvink D (2017) Assessing climate change impacts on the stability of small tidal inlets: part 1—data poor environments. *Mar Geodesy* 390:331–346. <https://doi.org/10.1016/j.margeo.2017.05.008>
- Fenster MS, Dolan R, Morton RA (2001) Coastal storms and shoreline change: signal or noise? *J Coast Res* 17:714–720
- Fitzgerald DM (1988) Shoreline erosional-depositional processes associated with tidal inlets. In: Aubrey DG, Weishar L (eds) *Hydrodynamics and sediment dynamics of tidal inlets*. Springer, New York, pp 186–225. [https://doi.org/10.1007/978-1-4757-4057-8\\_11](https://doi.org/10.1007/978-1-4757-4057-8_11)
- Flor-Blanco G, Alcántara-Carrió J, Jackson DWT, Flor G, Flores-Soriano C (2021) Coastal erosion in NW Spain: recent patterns under extreme storm wave events. *Geomorphology* 387:107767. <https://doi.org/10.1016/j.geomorph.2021.107767>
- Gens R (2010) Remote sensing of coastlines: detection, extraction and monitoring. *Int J Remote Sens* 31(7):1819–1836. <https://doi.org/10.1080/01431160902926673>
- Goncalves RM, Awange JL (2017) Three most widely used GNSS-based shoreline monitoring methods to support integrated coastal zone management policies. *J Surv Eng* 143(3):5017003. [https://doi.org/10.1061/\(ASCE\)SU.1943-5428.0000219](https://doi.org/10.1061/(ASCE)SU.1943-5428.0000219)
- Guisado-Pintado E, Jackson DWT (2018) Multi-scale variability of storm Ophelia 2017: the importance of synchronised environmental variables in coastal impact. *Sci Total Environ* 630:287–301. <https://doi.org/10.1016/j.scitotenv.2018.02.188>
- Gunasinghe GP, Ruhunage L, Ratnayake NP, Ratnayake AS, Samaradivakara GVI, Jayaratne R (2021) Influence of manmade effects on geomorphology, bathymetry and coastal dynamics in a monsoon-affected river outlet in Southwest Coast of Sri Lanka. *Environ Earth Sci* 80(7):1–16. <https://doi.org/10.1007/s12665-021-09555-0>
- Harris ME, Ellis JT, Barrineau P (2020) Evaluating the geomorphic response from sand fences on dunes impacted by hurricanes. *Ocean Coast Manag* 193:105–247. <https://doi.org/10.1016/j.ocecoaman.2020.105247>
- Hayes MO (1991) Geomorphology and sedimentation patterns of tidal inlets: a review. In: Kraus NC, Gingerich KJ, Kriebel DL (eds) *Coastal sediments '91*, American Society of Civil Engineers, New York, pp 1343–1355
- Héquette A, Ruz M, Zemmour A, Marin D, Cartier A, Sipka V (2019) Alongshore variability in coastal dune erosion and post-storm recovery, Northern Coast of France. *J Coast Res* 88(SI):25–45. <https://doi.org/10.2112/SI88-004.1>
- Immitzer M, Böck S, Einzmann K, Vuolo F, Pinnel N, Wallner A, Atzberger C (2018) Fractional cover mapping of spruce and pine at 1 Ha resolution combining very high and medium spatial resolution satellite imagery. *Remote Sens Environ* 204:690–703. <https://doi.org/10.1016/j.rse.2017.09.031>



- Jayathillake D (2020) Mount Lavinia beach nourishment project successful—DG Coastal Conservation Department. [http://www.defence.lk/Article/view\\_article/1679](http://www.defence.lk/Article/view_article/1679). Accessed 07 May 2021
- Kumar A, Jayappa K (2009) Long and short-term shoreline changes along Mangalore coast, India. *Int J Environ Res* 3:177–188
- Lee HJ (2014) A review of sediment dynamical processes in the west coast of Korea, eastern Yellow Sea. *Ocean Sci J* 49(2):85–95. <https://doi.org/10.1007/s12601-014-0010-0>
- Lee JS, Baek JY, Jung D, Shim JS, Lim HS, Jo YH (2019) Estimate of coastal water depth based on aerial photographs using a low-altitude remote sensing system. *Ocean Sci J* 54(3):349–362. <https://doi.org/10.1007/s12601-019-0026-6>
- Li R, Liu J, Felus Y (2001) Spatial modeling and analysis for shoreline change detection and coastal erosion monitoring. *Mar Geod* 24(1):1–12. <https://doi.org/10.1080/01490410121502>
- Li R, Ma R, Di K (2002) Digital tide-coordinated shoreline. *Mar Geod* 25(1–2):27–36. <https://doi.org/10.1080/014904102753516714>
- Miles JR, Russell PE (2004) Dynamics of a reflective beach with a low tide terrace. *Cont Shelf Res* 24(11):1219–1247. <https://doi.org/10.1016/j.csr.2004.03.004>
- Mitri G, Nader M, Dagher MA, Gebrael K (2020) Investigating the performance of sentinel-2A and landsat 8 imagery in mapping shoreline changes. *J Coast Conserv* 24(3):1–9. <https://doi.org/10.1007/s11852-020-00758-4>
- Natesan U, Thulasiraman N, Deepthi K, Kathiravan K (2013) Shoreline change analysis of Vedaranyam Coast, Tamil Nadu. *India Environ Monit Assess* 185(6):5099–5109. <https://doi.org/10.1007/s10661-012-2928-y>
- Nayananda OK (2007) The study of economic significance of coastal region of Sri Lanka in the context of environmental changes of pre and post tsunami. Coastal Conservation Department, The Ministry of Environment and Natural Resources, Sri Lanka
- Niya AK, Alesheikh AA, Soltanpor M, Kheirkhahzarkesh MM (2013) Shoreline change mapping using remote sensing and GIS. *IJRSA* 3(3):102–107
- Oertel GF (1988) Processes of sediment exchange between tidal inlets, ebb deltas and barrier islands. In: Aubrey DG, Weishar L (eds) *Hydrodynamics and sediment dynamics of tidal inlets*. Springer, New York, pp 297–318
- Palamakumbure L, Ratnayake AS, Premasiri HMR, Ratnayake NP, Katupotha J, Dushyantha N, Weththasinghe S, Weerakoon WAP (2020) Sea-level inundation and risk assessment along the south and southwest coasts of Sri Lanka. *Geoenviron Disast* 7(1):1–9. <https://doi.org/10.1186/s40677-020-00154-y>
- Parrish C, Sault M, White SA, Sellars J (2005) Empirical analysis of aerial camera filters for shoreline mapping. In: ASPRS 2005 annual conference "geospatial goes global: from your neighborhood to the whole planet", American Society for Photogrammetry and Remote Sensing, Baltimore, Maryland, 7–11 Mar 2005
- Pattiaratchi C, Azmy N, de Vos A (2020) The tragedy of Mount Lavinia beach. <https://oceanswell.org/books-reports/the-tragedy-of-mount-lavinia-beach> Accessed 8 May 2021
- Pinet PR (2019) *Invitation to oceanography*. Jones & Bartlett Learning, Sudbury, p 230
- Rajith K, Kurian NP, Thomas KV, Prakash TN, Hameed TSS (2008) Erosion and accretion of a placer mining beach of SW Indian Coast. *Mar Geod* 31(2):128–142. <https://doi.org/10.1080/01490410802092136>
- Ratnayake NP, Silva KBA, Kumara IGIK (2013) Chloride contamination in construction aggregates due to periodic saline water intrusion: a case study in the Kaluganga River Estuary, Sri Lanka. *Environ Earth Sci* 69(8):2529–2540. <https://doi.org/10.1007/s12665-012-2077-1>
- Ratnayake NP, Ratnayake AS, Keegle PV, MallawaArachchi MAKM, Premasiri HMR (2018) An analysis of beach profile changes subsequent to the colombo Harbor Expansion project, Sri Lanka. *Environ Earth Sci* 77(1):1–11. <https://doi.org/10.1007/s12665-018-7234-8>
- Ratnayake NP, Ratnayake AS, Azoor RM, Weththasinghe SM, Senarathne IDJ, Premasiri R, Dushyantha N (2019) Erosion processes driven by monsoon events after a beach nourishment and breakwater construction at Uswetakeiyawa Beach, Sri Lanka. *SN Appl Sci* 1(1):1–11. <https://doi.org/10.1007/s42452-018-0050-7>
- Ruggiero P, Komar PD, McDougal WG, Marra JJ, Beach RA (2001) Wave runup, extreme water levels and the erosion of properties backing beaches. *J Coast Res* 17(2):407–419
- Saleem A, Awange JL (2019) Coastline shift analysis in data deficient regions: exploiting the high spatio-temporal resolution sentinel-2 products. *Catena* 179:6–19. <https://doi.org/10.1016/j.catena.2019.03.023>
- Samarasekara RSM, Sasaki J, Jayaratne R, Suzuki T, Ranawaka RAS, Pathmasiri SD (2018) Historical changes in the shoreline and management of Marawila Beach, Sri Lanka, from 1980 to 2017. *Ocean Coast Manag* 165:370–384. <https://doi.org/10.1016/j.ocecoaman.2018.09.012>
- Scott DB (2005) Coastal Changes, Rapid. In: Finkl CW, Makowski C (eds) *Encyclopedia of coastal sciences*. Springer, Cham, pp 253–255
- Specht M, Specht C, Lewicka O, Makar A, Burdziakowski P, Dąbrowski P (2020) Study on the coastline evolution in sopot (2008–2018) based on landsat satellite imagery. *J Mar Sci Eng* 8(6):464. <https://doi.org/10.3390/jmse8060464>
- Srisangeerthan S (2015) Tropical cyclone damages in Sri Lanka. *Wind Eng JAWE* 40(3):294–302. <https://doi.org/10.5359/jawe.40.294>
- Topouzelis K, Spondylidis SC, Papakonstantinou A, Soulakellis N (2016) The use of sentinel-2 imagery for seagrass mapping: Kalloni Gulf (Lesvos Island, Greece) case study. In: Fourth international conference on remote sensing and geoinformation of the environment 2016, International Society for Optics and Photonics, Paphos, Cyprus, 4–8 April 2016
- Vos K, Splinter KD, Harley MD, Simmons JA, Turner IL (2019a) CoastSat: a google earth engine-enabled python toolkit to extract shorelines from publicly available satellite imagery. *Environ Model Softw* 122:104528. <https://doi.org/10.1016/j.envsoft.2019.104528>
- Vos K, Harley MD, Splinter KD, Simmons JA, Turner IL (2019b) Sub-annual to multi-decadal shoreline variability from publicly available satellite imagery. *Coast Eng* 150:160–174. <https://doi.org/10.1016/j.coastaleng.2019.04.004>
- Warnasuriya TWS, Gunaalan K, Gunasekara SS (2018) Google Earth: a new resource for shoreline change estimation—case study from Jaffna Peninsula, Sri Lanka. *Mar Geod* 41(6):546–580. <https://doi.org/10.1080/01490419.2018.1509160>
- Warnasuriya TWS, Kumara PBTP, Alahacoon N (2015) Mapping of selected coral reefs in Southern, Sri Lanka using remote sensing methods, Sri Lanka. *J Aquat Sci* 19:41–55. <https://doi.org/10.4038/sljias.v19i0.7450>
- Weththasinghe DSM, Ratnayake NP, Hemalal PVA, Dushyantha NP (2021) Enhancing scientific and societal understanding of geohazards in Sri Lanka. In: Dilek Y, Ogawa Y, Okubo Y (eds) *Characterization of modern and historical seismic–tsunami events, and their global–societal impacts*. Geological Society, London, Special Publications, pp 367–380. <https://doi.org/10.1144/SP501-2018-177>
- Yang X, Li J (2012) *Advances in mapping from remote sensor imagery: techniques and applications*. CRC Press, Boca Raton, p 464
- Yang L, Dong Y (2017) Research progress of coastal dunes response to storm. *Adv Earth Sci* 32(7):716–722
- Yu K, Hu C, Muller-Karger FE, Lu D, Soto I (2011) Shoreline changes in West-Central Florida between 1987 and 2008 from landsat

observations. *Int J Remote Sens* 32(23):8299–8313. <https://doi.org/10.1080/01431161.2010.535045>

Zhang K, Douglas BC, Leatherman SP (2004) Global warming and coastal erosion. *Clim Change* 64(1):41–58. <https://doi.org/10.1023/B:CLIM.0000024690.32682.48>

**Publisher's Note** Springer Nature remains neutral with regard to jurisdictional claims in published maps and institutional affiliations.